Supporting Information

Hong et al. 10.1073/pnas.1305235110

SI Materials and Methods

Behavioral Procedures. All procedures were approved by the Institute of Laboratory Animal Resources of Seoul National University. Male Sprague–Dawley rats (4-5 wk old) were maintained with free access to food and water under an inverted 12-h/12-h light/dark cycle (lights off at 0900 hours). Behavioral training was performed in the dark portion of the cycle. For fear conditioning, rats were placed in a Plexiglas conditioning chamber (Coulbourn Instruments) and left undisturbed for 2 min. Then a neutral tone (30 s, 2.8 kHz, 85 dB sound pressure level) coterminating with an electrical foot shock (1.0 mA, 1 s) was presented three times at an average interval of 100 s. For behavioral experiments, a shock intensity of 0.7 mA or 0.5 mA was used, to avoid fear saturation. Rats were returned to their home cage at 60 s after the last shock had been applied. A chamber distinct from the conditioning chamber was used for both the retrieval (reactivation) and retention tests. Tone tests (both retrieval and retention tests) consisted of single nonreinforced tone presentations. Context exposure control animals were exposed to the same context for an identical duration without the tone presentation. The reconditioning procedure followed the protocol for conditioning, but in a third context. Conditioned freezing was defined as immobility except for respiratory movements, and was quantified by trained observers who were blinded to the experimental groups. Total freezing time during a test period was normalized to the duration of either the tone presentation (30 s) or the context exposure.

Animal Surgery and Histology. Rats were anesthetized with sodium pentobarbital (50 mg/kg i.p.). When fully anesthetized, rats were mounted on a stereotaxic apparatus (David Kopf Instruments) and implanted bilaterally into the lateral amygdala (LA; anteroposterior, −2.3 mm; mediolateral, ±4.9 mm; dorsoventral, −6.5 mm from bregma) with 26-gauge stainless steel cannulas (model C315G; Plastic Products). A 32-gauge dummy cannula was inserted into each guide cannula to prevent clogging. Two jewelry screws were implanted over the skull to serve as anchors, and the whole assembly was affixed to the skull with dental cement. Rats were given at least 5 d to recover before experiments. To verify the intra-LA placement of the injector cannula tips, rats were anesthetized after completion of the experiments with urethane (1 g/kg, i.p.) and transcardially perfused with 0.9% saline solution, followed by 10% buffered formalin. Brains were removed and postfixed overnight. Coronal sections (80 μm thick) were cut with a vibroslicer (NVSL; World Precision Instruments), stained with cresyl-violet, and examined under light microscopy.

Intra-Amygdala Infusion. Anisomycin (Sigma-Aldrich) was dissolved in equimolar HCl, diluted with artificial cerebrospinal fluid (aCSF), and adjusted to pH 7.4 with NaOH (1). 1-Naphthylacetylsperimine (NASPM; Sigma-Aldrich) was dissolved in 90% PBS/10% DMSO. D-(-)-2-amino-5-phosphonopentanoic acid (D-AP5) (Sigma-Aldrich), Tat-GluA2^{3Y} [Tat-GluR2^{3Y}, TAT(47–57)-869YKEGYNVYG877], and Tat-GluA2$_{3Y}$ [Tat-GluR2$_{3Y}$, TAT(47–57)-AKEGANVAG] peptides (2–4) (Peptron) were dissolved in aCSF. Anisomycin (62.5 μg/0.5 μL/side), NASPM (5, 6) (4 μg/0.5 μL/side or 0.4 μg/0.5 μL/side), D-AP5 (7) (2.5 μg/0.5 μL/side), or peptides (25 pmol/0.5 μL/side) were administrated bilaterally into the LA via a 33-gauge injector cannula (C315I; Plastic Products) attached to a 10-μL Hamilton syringe at a rate of 0.25 μL/min. After drug infusion, the injector cannulas were left in place for an additional 1 min to allow the drug to diffuse away from the cannula tip. Dummy cannulas were then swapped in, and the rats were returned to their home cages.

Slice Preparation. Electrophysiological experiments were carried out regularly at a fixed time of the day on age-matched rats to avoid circadian variation and developmental fluctuations of calcium-permeable AMPA receptors (CP-AMPARs) (8–10). To prevent bias, the experimenter was blinded to the behavioral group whenever possible. Brain slices were prepared using techniques described previously (4, 11). In brief, Sprague–Dawley rats (4-5 wk old) were rapidly anesthetized with halothane and then decapitated. The isolated whole brains were placed in an ice-cold modified aCSF solution containing 175 mM sucrose, 20 mM NaCl, 3.5 mM KCl, 1.25 mM NaH_2PO_4, 26 mM $NaHCO_3$, 1.3 mM $MgCl_2$, and 11 mM D-(+)-glucose and gassed with 95% O_2/5% CO_2. Coronal slices (300 μm) including the LA were cut using a vibroslicer (Campden Instruments) and incubated in normal aCSF containing 120 mM NaCl, 3.5 mM KCl, 1.25 mM NaH_2PO_4, 26 mM $NaHCO_3$, 1.3 mM $MgCl_2$, 2 mM $CaCl_2$, and 11 mM D-(+)-glucose and continuously bubbled at room temperature with 95% O_2/5% CO_2. Immediately before a slice was transferred to the recording chamber, the cortex overlying the LA was cut away with a scalpel, so that cortical epileptic burst discharges would not invade the LA in the presence of picrotoxin.

Recording Conditions. Whole-cell recordings were performed with borosilicate electrodes (2.0–3.5 MΩ) from visually identified pyramidal neurons in the dorsolateral division of the LA. The cells were classified as principal neurons based on the pyramidal shape of their somata. During voltage-clamping, a minor proportion (<5%) of recorded neurons exhibited spontaneous excitatory postsynaptic currents (EPSCs) with faster decay times and larger amplitude (>100 pA), characteristics typical of interneurons in the LA (12, 13), and were excluded from our analysis (4). Picrotoxin (100 μM; Sigma-Aldrich) was included in the recording solution to isolate excitatory synaptic transmission and block feed-forward GABAergic inputs to principal neurons in the LA.

Afferent Stimulation. We used brain slices containing well-isolated, sharply defined trunks (with thalamic afferents) innervating the dorsolateral division of the LA, where somatosensory and auditory inputs are known to converge (14). The sizes of the LA and central amygdala were relatively constant in these slices, and the fiber bundles closest to the central nucleus of the amygdala were used when multiple fibers were observed. Thalamic afferents were stimulated using a concentric bipolar electrode (MCE-100; Rhodes Medical Instruments) placed on the fiber bundle at the midpoint between the internal capsule and the medial boundary of the LA (4). When feasible, two distinct fiber bundles were stimulated in an alternating fashion, and linear additivity was tested to verify independent synaptic inputs. No systematic differences of stimulation pathway were detected in observed measures, so the results were pooled. Monosynaptic responses were judged on their latency, which was 3–4 ms on average and remained constant throughout the experiments.

Whole-Cell Patch-Clamp Recordings. Whole-cell recordings were made using a MultiClamp 700A/B (Molecular Devices). Recordings were obtained using pipettes with resistance of 2.0–3.5 MΩ when filled with the following solution: 100 mM Cs-gluconate, 0.6 mM EGTA, 10 mM Hepes, 5 mM NaCl, 20 mM tetraethylammonium (TEA), 4 mM Mg-ATP, 0.3 mM Na-GTP, and

3 mM QX314, with pH adjusted to 7.2 with CsOH and osmolarity adjusted to ~297 mmol/kg with sucrose. A junction potential of ~ –10 mV was left uncorrected. Recordings were made under infrared differential interference contrast (IR-DIC)–enhanced visual guidance from neurons that were three to four cell layers below the surface of the 300 μm slices at 32.0 ± 0.5 °C. Neurons were voltage-clamped at –70 mV, and solutions were delivered to slices via superfusion driven at a flow rate of 1.5 mL/min. The pipette series resistance was monitored throughout the experiments, and if it changed by >20%, the data were discarded. Whole-cell currents were filtered at 10 kHz, digitized at 20 kHz, and stored on a microcomputer (Clampex 8 software; Molecular Devices). For the purposes of presentation, running averages of four data points were applied in the time-lapse experiments.

AMPA/NMDA ratios were calculated as the ratio of the peak current at –70 mV to the current at 100 ms after stimulus onset at +40 mV. (AMPAR currents make a negligible contribution at this interval, as verified by D-AP5 treatment.) No systematic effects of conditioning or retrieval on the kinetics of NMDA receptor (NMDAR) currents were detected. The rectification index was calculated as a ratio of the slopes of a linear fit of 11 current-voltage (I-V) points, in which the index = [slope at negative holding potentials (–70 to 0 mV)] divided by the [slope at positive holding potentials (+30 to +50 mV)]. Accordingly, an index of 1 represents perfect linearity, whereas values >1 indicate inward rectification (12, 15, 16). NASPM (50 μM) was used to detect CP-AMPARs in the presence of D-AP5 (50 μM). Miniature EPSCs (mEPSCs) were recorded in the presence of TTX (1 μM) and analyzed with MiniAnalysis (Synaptosoft) using a detection threshold of 7 pA (>2 times root mean square noise). Decay times were obtained by single-exponential fitting of the average mEPSC traces.

Whole-Cell Recordings in Cannulated Rats. To determine the molecular mechanisms involved in the calcium-impermeable AMPA receptor CI-AMPAR–to–CP-AMPAR exchange on memory retrieval, we combined in vivo behavioral manipulations and drug microinfusion in cannulated rats with ex vivo whole-cell recordings. After drug infusion and behavioral manipulation, rats were rapidly anesthetized and then decapitated. Cannula placement was confirmed during slice preparation, and microscopic images were obtained to guide subsequent whole-cell recordings. Recordings were made in slices directly adjacent to the slice containing the injection cannula trajectory site, resulting in recordings within 500 μm of the infusion site. To test the efficacy of drug delivery, we injected the irreversible, use-dependent NMDAR antagonist MK-801 into the LA and prepared slices 30 min later, and found severely impaired NMDAR transmission (Fig. S4). These results confirm the in vivo efficacy of drug microinfusion, and also suggest that LA synapses undergo significant basal activity, even in the absence of behavioral manipulation.

Statistical Analysis. The results comparing single data points between behavior-trained groups were analyzed using an unpaired *t* test for comparison of two treatment groups or one-way ANOVA with subsequent Newman–Keuls post hoc comparison for more than two treatment groups. Two-way ANOVA (repeated-measures) and subsequent Bonferroni post hoc comparison were used for the analysis of retrieval and reconsolidation. In the time-lapse electrophysiological experiments, a temporal average of the data points during a period of interest was used for statistical comparison of EPSCs (5 min). A P value < 0.05 was considered to indicate statistical significance.

Nomenclature. CP-AMPARs consist mainly of GluA2-lacking AMPARs, but also include AMPARs consisting of GluA2 subunits with an unedited Q/R site glutamine residue in the channel pore (17, 18). mRNA editing leads to the incorporation of a charged arginine residue at this site of GluA2, which underlies the calcium impermeability and resistance to polyamine toxins of CI-AMPARs. Because the mRNA editing of GluA2 in rats is almost complete by adolescence, and the contribution of other calcium-permeable glutamate receptors, such as kainate receptors, to LA synaptic transmission is marginal (19), we refer to CI-AMPARs as GluA2-containing AMPARs.

Because CP-AMPARs have higher conductance than CI-AMPARs, the CI-AMPAR–to–CP-AMPAR exchange that we describe here is not a one-for-one exchange, but rather an equiconductance exchange. Such one-for-one exchanges have been implicated in other studies in which synaptic strength changes (15, 20), and thus likely involve other mechanisms.

1. Nader K, Schafe GE, Le Doux JE (2000) Fear memories require protein synthesis in the amygdala for reconsolidation after retrieval. *Nature* 406(6797):722–726.
2. Ahmadian G, et al. (2004) Tyrosine phosphorylation of GluR2 is required for insulin-stimulated AMPA receptor endocytosis and LTD. *EMBO J* 23(5):1040–1050.
3. Brebner K, et al. (2005) Nucleus accumbens long-term depression and the expression of behavioral sensitization. *Science* 310(5752):1340–1343.
4. Kim J, et al. (2007) Amygdala depotentiation and fear extinction. *Proc Natl Acad Sci USA* 104(52):20955–20960.
5. Conrad KL, et al. (2008) Formation of accumbens GluR2-lacking AMPA receptors mediates incubation of cocaine craving. *Nature* 454(7200):118–121.
6. Noh KM, et al. (2005) Blockade of calcium-permeable AMPA receptors protects hippocampal neurons against global ischemia-induced death. *Proc Natl Acad Sci USA* 102(34):12230–12235.
7. Ben Mamou C, Gamache K, Nader K (2006) NMDA receptors are critical for unleashing consolidated auditory fear memories. *Nat Neurosci* 9(10):1237–1239.
8. Lanté F, Toledo-Salas JC, Ondrejcak T, Rowan MJ, Ulrich D (2011) Removal of synaptic Ca^{2+}-permeable AMPA receptors during sleep. *J Neurosci* 31(11):3953–3961.
9. Vyazovskiy VV, Cirelli C, Pfister-Genskow M, Faraguna U, Tononi G (2008) Molecular and electrophysiological evidence for net synaptic potentiation in wake and depression in sleep. *Nat Neurosci* 11(2):200–208.
10. Collingridge GL, Peineau S, Howland JG, Wang YT (2010) Long-term depression in the CNS. *Nat Rev Neurosci* 11(7):459–473.
11. Choi S, Klingauf J, Tsien RW (2000) Postfusional regulation of cleft glutamate concentration during LTP at "silent synapses." *Nat Neurosci* 3(4):330–336.
12. Mahanty NK, Sah P (1998) Calcium-permeable AMPA receptors mediate long-term potentiation in interneurons in the amygdala. *Nature* 394(6694):683–687.
13. Sah P, Lopez De Armentia M (2003) Excitatory synaptic transmission in the lateral and central amygdala. *Ann N Y Acad Sci* 985:67–77.
14. Pitkänen A, Savander V, LeDoux JE (1997) Organization of intra-amygdaloid circuitries in the rat: An emerging framework for understanding functions of the amygdala. *Trends Neurosci* 20(11):517–523.
15. Liu SQ, Cull-Candy SG (2000) Synaptic activity at calcium-permeable AMPA receptors induces a switch in receptor subtype. *Nature* 405(6785):454–458.
16. Clem RL, Huganir RL (2010) Calcium-permeable AMPA receptor dynamics mediate fear memory erasure. *Science* 330(6007):1108–1112.
17. Cull-Candy S, Kelly L, Farrant M (2006) Regulation of $Ca2^{+}$-permeable AMPA receptors: Synaptic plasticity and beyond. *Curr Opin Neurobiol* 16(3):288–297.
18. Kwak S, Weiss JH (2006) Calcium-permeable AMPA channels in neurodegenerative disease and ischemia. *Curr Opin Neurobiol* 16(3):281–287.
19. Rogan M, Stäubli U, LeDoux J (1997) Fear conditioning induces associative long-term potentiation in the amygdala. *Nature* 390(6660):604–607.
20. Mameli M, Balland B, Luján R, Lüscher C (2007) Rapid synthesis and synaptic insertion of GluR2 for mGluR-LTD in the ventral tegmental area. *Science* 317(5837):530–533.

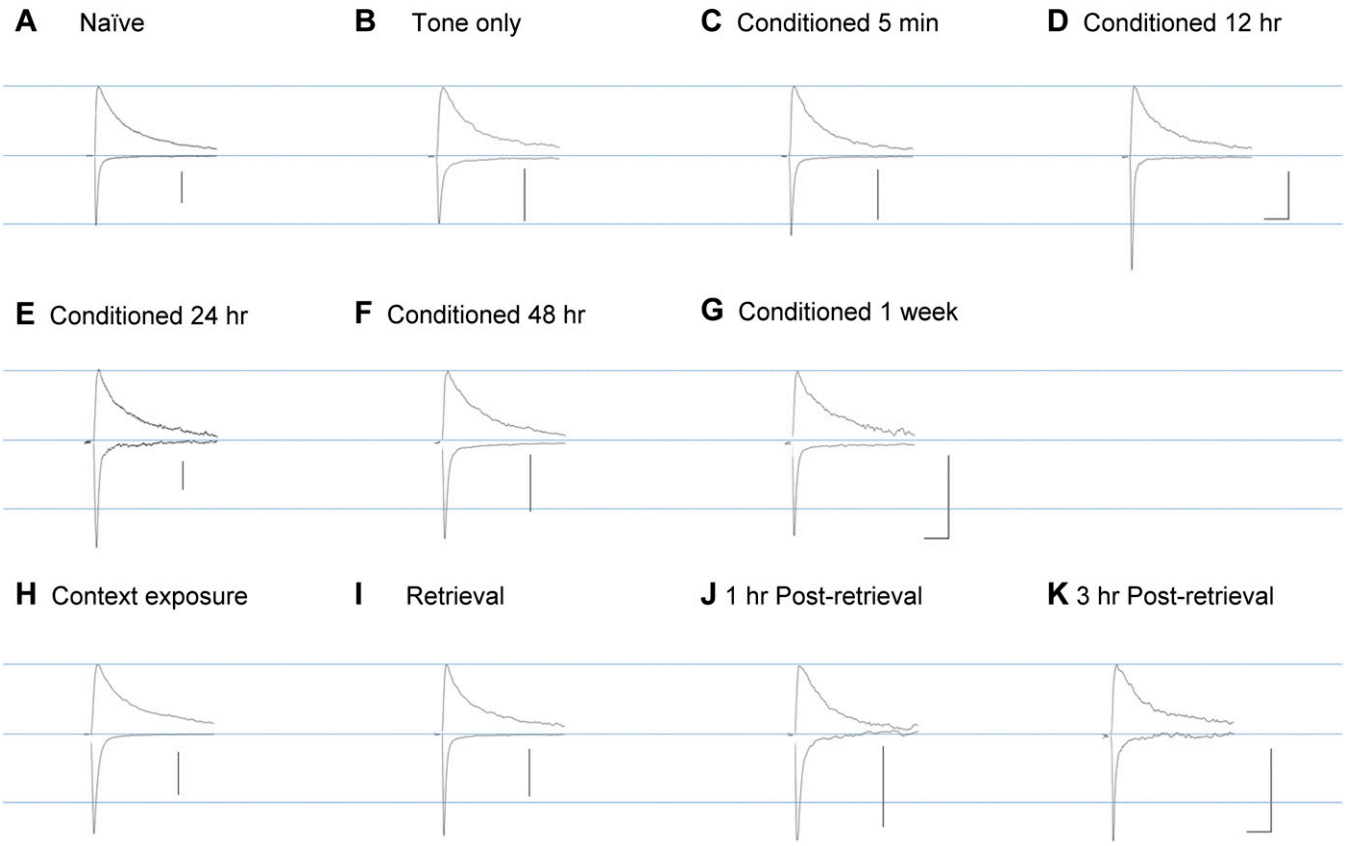

Fig. S1. Fear conditioning significantly potentiates the AMPAR/NMDAR-EPSC ratio in the LA, whereas fear memory retrieval has no effect. (*A*–*K*) Representative AMPAR/NMDAR-EPSCs at membrane holding potentials, V_h, of −70 and +40 mV during stimulation of thalamo-amygdala synapses from rats subjected to fear conditioning and memory retrieval before slice preparation. (Scale bars: 100 pA and 50 ms.)

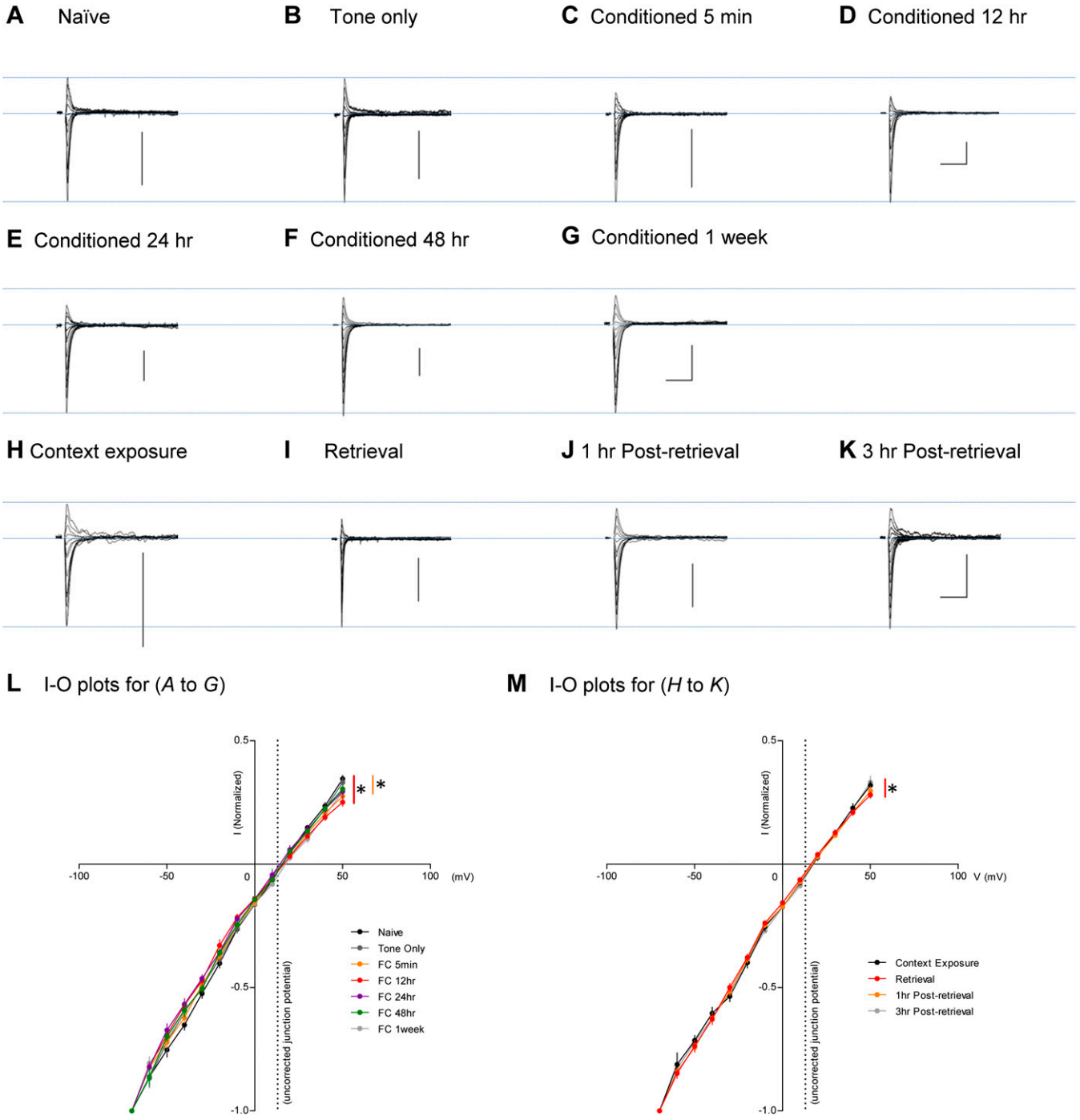

Fig. S2. Both fear conditioning and fear memory retrieval induce a transient increase in AMPAR rectification in the LA. (*A–K*) Representative AMPAR-EPSCs at membrane holding potentials, V_h, of −70 ∼+50 mV during stimulation of thalamo-amygdala synapses from rats subjected to fear conditioning and memory retrieval before slice preparation. (Scale bars: 100 pA and 50 ms.) (*L* and *M*) Normalized I-V plots were constructed from peak amplitudes of AMPAR-EPSCs at varying intervals after learning and retrieval.

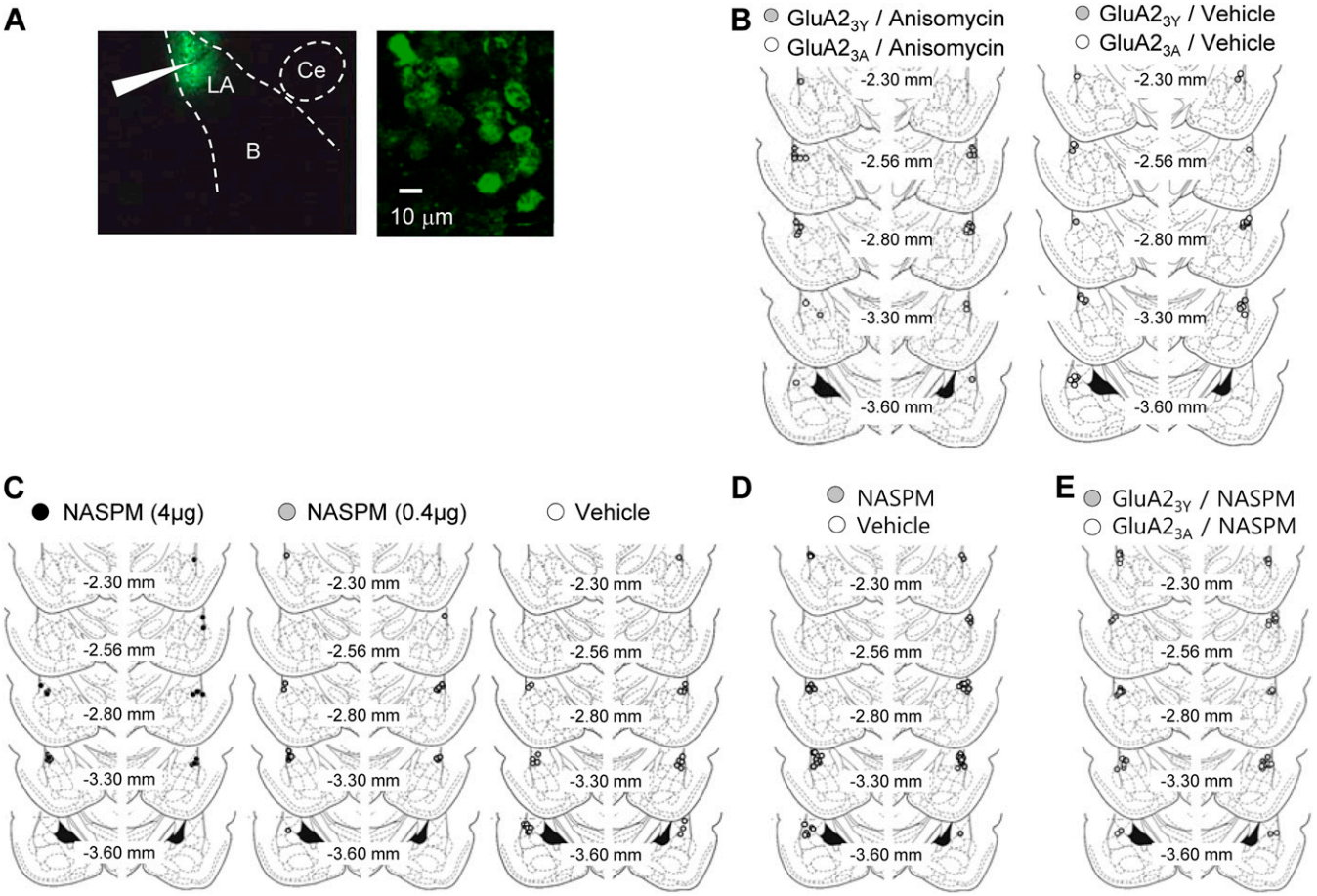

Fig. S3. Diffusion of the microinjected peptide and schematic illustrations of cannula tip placement. (*A*) (*Left*) Diffusion of the fluorescent dansyl-Tat-GluA2$_{3Y}$ peptide (1.5 nmol) within 1 h after microinjection, as visualized with a multiphoton microscope (the flattened image of 10 optical sections; $\triangle z = 10$ mm). The white arrow indicates the end of the injector cannula. (*Right*) Peptide transduction in individual LA neurons at high magnification. LA, lateral nucleus; B, basal nucleus; CE, central nucleus. (*B*) Schematic illustration showing cannula tip placement for experiments in Fig. 2*B*, *Left* (GluA2$_{3Y}$/anisomycin, gray circle; GluA2$_{3A}$/anisomycin, open circle), and Fig. 2*C*, *Right* (GluA2$_{3Y}$/vehicle, gray circle; GluA2$_{3A}$/vehicle, open circle). The illustration was based on drawings in Paxinos and Watson (1). (*C*) Schematic illustrations showing the cannula tip placement in the experiments shown in Fig. 4 *B* and *C* (high-dose NASPM, black circle; low-dose NASPM, gray circle; vehicle, open circle). (*D*) Schematic illustrations showing cannula tip placement in the experiments shown in Fig. 4*D* (NASPM, gray circle; vehicle, open circle). (*E*) Schematic illustrations showing the cannula tip placement in the experiments shown in Fig. 4*F* (GluA2$_{3Y}$/NASPM, gray circle; GluA2$_{3A}$/NASPM, open circle).

1. Paxinos G, Watson C (1998) *The Rat Brain in Stereotaxic Coordinates* (Academic, San Diego).

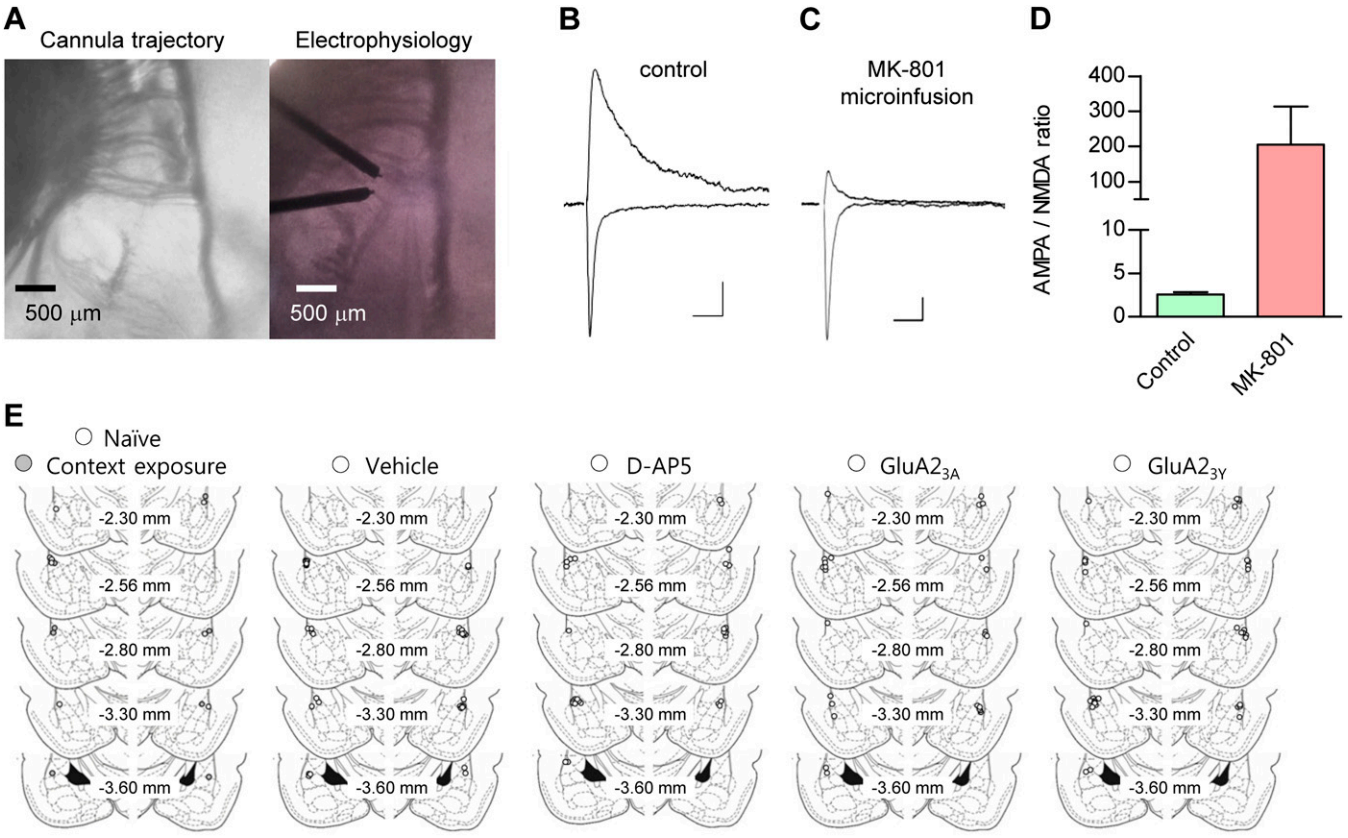

Fig. S4. Whole-cell recordings in cannulated rats. *(A)* Representative microscope images showing cannula tip placement and whole-cell recordings in adjacent slices for experiments. (*B*) Control (no previous drug infusion) AMPA/NMDA currents from neurons within 500 μm of the infusion site (infusion cannula tip) in cannulated rat brain amygdala slices. (Scale bars: 50 ms and 20 pA.) (*C*) Increased AMPA/NMDA ratio in brain slices from rats microinfused bilaterally with NMDAR antagonist MK-801 (15 nmol/0.5 μL/side) at 30 min before decapitation. (*D*) Summarized results. (*E*) Schematic illustration showing cannula tip placement for the experiments shown in Fig. 3 *B–H*.

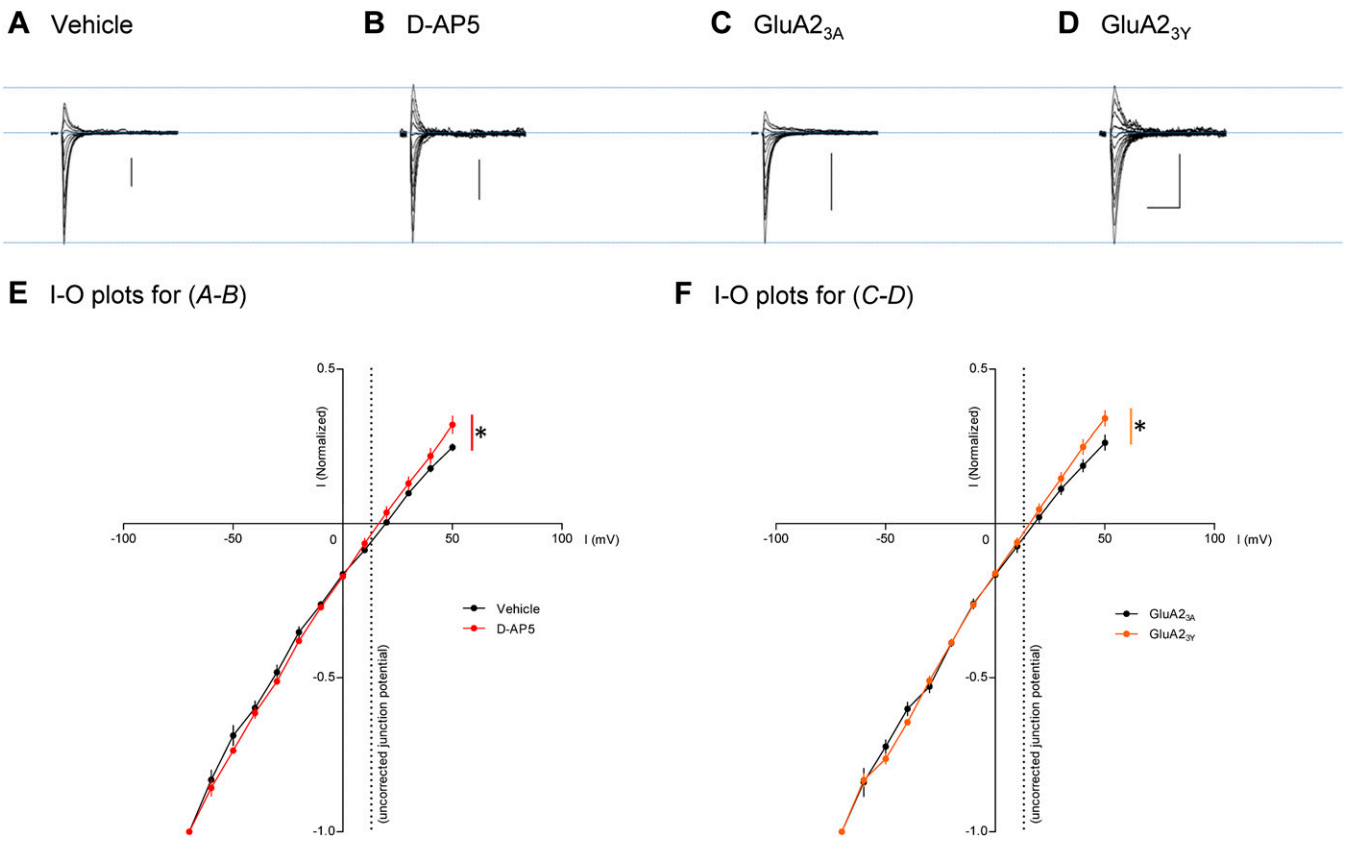

Fig. S5. Transient increase of AMPAR rectification induced by fear memory retrieval requires NMDAR activity and GluA2-containing AMPAR endocytosis. (*A–D*) Representative AMPAR-EPSCs at membrane holding potentials, V_h, of −70~+50 mV during stimulation of thalamo-amygdala synapses from rats subjected to cannula infusion and fear memory retrieval before slice preparation. (Scale bars: 100 pA and 50 ms.) (*E* and *F*) Normalized I-V plots constructed from peak amplitude of AMPAR-EPSCs after drug infusion and fear memory retrieval.

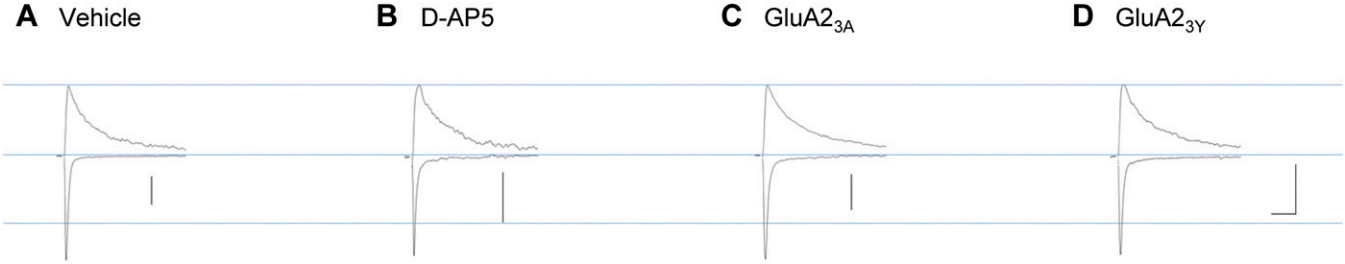

Fig. S6. Memory retrieval after D-AP5 or GluA2$_{3Y}$ infusion has no effect on AMPAR/NMDAR-EPSC ratio in the LA. (*A–D*) Representative AMPAR/NMDAR-EPSCs at membrane holding potentials, V_h, of −70 and +40 mV during stimulation of thalamo-amygdala synapses from rats subjected to cannula infusion and fear memory retrieval before slice preparation. (Scale bars: 100 pA and 50 ms.)

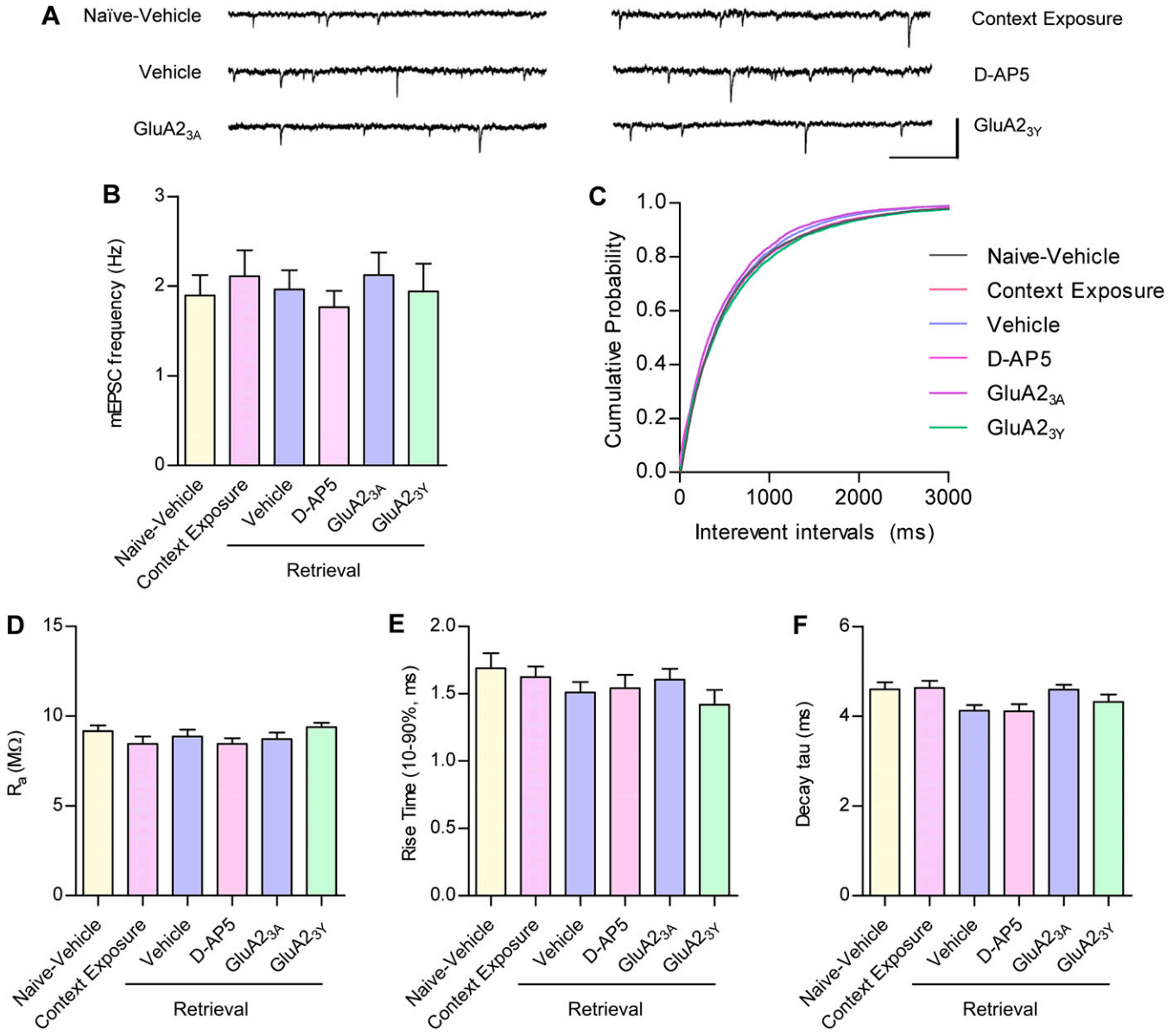

Fig. S7. Effect of fear memory acquisition and retrieval on AMPAR-mEPSCs in the LA. (*A*) Sample traces of AMPAR-mEPSCs recorded in LA neurons from behavior- and drug-treated rats. AMPAR-mEPSCs were recorded in the presence of TTX (1 μM), D-AP5 (50 μM), and picrotoxin (100 μM) to isolate AMPAR transmission on spontaneous miniature events. (Scale bars: 50 pA and 200 ms.) (*B* and *C*) Bar graph of AMPAR-mEPSC frequency (*B*) and cumulative histogram of interevent interval (*C*). mEPSC frequency was not different among the groups examined (naïve-vehicle, 1.89 ± 0.23 Hz; context exposure-vehicle, 2.11 ± 0.29 Hz; vehicle, 1.96 ± 0.21 Hz; D-AP5, 1.77 ± 0.18 Hz; GluA2$_{3A}$, 2.12 ± 0.25 Hz; GluA2$_{3Y}$, 1.94 ± 0.31 Hz; $F_{5,84} = 0.3776$, $P > 0.05$, one-way ANOVA; $P > 0.05$ for all pairs, Newman–Keuls post hoc test). (*D–F*) Access resistance, rise time, and decay time of AMPAR-mEPSCs showed no significant differences among groups.